Identification and functional analysis of SOX10 missense mutations in different subtypes of Waardenburg syndrome.

Asma Chaoui, Yuli Watanabe, Renaud Touraine, Viviane Baral, Michel Goossens, Véronique Pingault, Nadège Bondurand

Identification and functional analysis of SOX10 missense mutations in different subtypes of Waardenburg syndrome

Asma Chaoui[1,2#], Yuli Watanabe[1,2#], Renaud Touraine[3], Viviane Baral[1,2], Michel Goossens[1,2,4], Veronique Pingault[1,2,4], and Nadege Bondurand[1,2]*.

[1] INSERM, U955, Créteil, 94000, France ;

[2] Université Paris Est, Faculté de Médecine, Créteil, 94000, France ;

[3] CHU-Hôpital Nord, Service de Génétique, Saint Etienne, 42000, France ;

[4] AP-HP, Hôpital H. Mondor - A. Chenevier, Service de Biochimie et Génétique, Créteil, 94000, France.

[#] The authors wish it to be known that, in their opinion, the first two authors should be regarded as joint first authors.

* Corresponding author. Nadège Bondurand. INSERM U955, Equipe 11, Hôpital Henri Mondor, 51 Avenue du Maréchal de Lattre de Tassigny, 94010, Créteil, France. Email: nadege.bondurand@inserm.fr; Tel: +33149812854. Fax: +33148993345

Abstract

Waardenburg syndrome (WS) is a rare disorder characterized by pigmentation defects and sensorineural deafness, classified into four clinical subtypes, WS1-4. Whereas the absence of additional features characterizes WS2, association with Hirschsprung's disease defines WS4. WS is genetically heterogeneous, with six genes already identified, including *SOX10*. About 50 heterozygous *SOX10* mutations have been described in patients presenting with WS2 or WS4, with or without myelination defects of the peripheral and central nervous system (PCWH or PCW). The majority are truncating mutations that most often remove the main functional domains of the protein. Only three missense mutations have been thus far reported. In the present study, novel SOX10 missense mutations were found in 11 patients and examined for effects on SOX10 characteristics and functions. The mutations were associated with various phenotypes, ranging from WS2 to PCWH. All tested mutations were found to be deleterious. Some mutants presented with partial cytoplasmic redistribution, some lost their DNA binding and/or transactivation capabilities on various tissue-specific target genes. Intriguingly, several mutants were redistributed in nuclear foci. Whether this phenomenon is a cause or a consequence of mutation-associated pathogenicity remains to be determined, but this observation could help to identify new SOX10 modes of action.

Keywords: Waardenburg syndrome; SOX10; neural crest, enteric nervous system, Hirschsprung's.

Introduction

Waardenburg syndrome (WS) is an auditory-pigmentary disorder with an incidence of one in 40,000 that manifests with sensorineural deafness and abnormal pigmentation of the hair, skin, and iris (Read and Newton, 1997). This syndrome results from an abnormal proliferation, survival, migration or differentiation of neural crest derived melanocytes and is therefore defined as a neurocristopathy (Bolande, 1974; Le Douarin and Kalcheim, 1999). WS is classified into four subtypes, WS1-4, depending on the presence of additional symptoms. The absence of additional features characterizes WS2 (MIM 193510, 611584). Facial dysmorphic features are present in WS1 and WS3 patients, whereas an association with Hirschsprung's disease (HD, aganglionic megacolon) defines WS4, also called Shah-Waardenburg syndrome or Waardenburg-Hirschsprung's disease (MIM 277580, 613265, 613266). HD is the main cause of congenital intestinal obstruction, with an incidence of one in 5,000 live births. It is characterized by the absence of enteric ganglia along a variable length of the intestine (Read and Newton, 1997; Amiel et al., 2008; Pingault et al., 2010).

WS is a genetically heterogeneous condition. Indeed, numerous heterozygous mutations in the genes encoding the PAX3, MITF, and SOX10 transcription factors, as well as homozygous or heterozygous mutations in the genes encoding endothelin-3 (*EDN3*) or endothelin-B receptor (*EDNRB*) have been reported (Pingault et al., 2010). Since 1998, about 50 heterozygous mutations or deletions of the *SOX10* gene have been described in WS patients (Pingault et al., 2010).

SOX10 belongs to the SOX (SRY related HMG box) family of transcription factors and is closely related to SOX8 and SOX9, the latter being involved in campomelic dysplasia (Foster et al., 1994; Wagner et al., 1994; Mollaaghababa and Pavan, 2003; Hong and Saint-Jeannet, 2005; Kelsh, 2006; Guth and Wegner, 2008). All SOX proteins are characterized by a highly conserved motif of 80 amino acids called the HMG (high mobility group) domain which

allows targeting of the DNA minor groove and recognition of a 7 bp consensus DNA element (Werner et al., 1995; Lefebvre et al., 2007; Malki et al., 2010). The HMG domain is made up of three α-helices that adopt an L-type shape. A hydrophobic core is formed at the intersection of the three helices to maintain the structural shape (Murphy et al., 2001; Li et al., 2006). The HMG domain also enables intracellular transport regulation (Malki et al., 2010). Indeed, it contains two distinct nuclear localization signals (NLSs) using calmodulin (for the N-terminal NLS) and β importins (for the C-terminal NLS) to drive the SOX proteins into the nucleus (Poulat et al., 1995; Sudbeck and Scherer, 1997; Malki et al., 2010). Sex reversal mutations have been independently described in both the N- and C-terminal NLSs of SRY and SOX9; both of these affect the subcellular location of the resulting proteins (Sim et al., 2008). Other sequences or post-translational modifications, such as phosphorylation, acetylation, and sumoylation, are also known to modulate the subcellular location of SOX factors (Lefebvre et al., 2007; Malki et al., 2010). Besides NLSs, a perfect nuclear export signal (NES) has been identified, suggesting active nucleocytoplasmic shuttling (Rehberg et al., 2002).

The distal part of the HMG domain of SOX10 (amino acids 133 to 203) is also involved in protein-protein interactions with its partners and may thus be crucial for synergistic regulation of gene expression (Wissmuller et al., 2006). DNA bindingSOX factors are known to regulate expression of a variety of genes through binding to their promoter or enhancer regions, either alone or in cooperation with various cofactors (Kamachi et al., 2000; Wilson and Koopman, 2002; Bernard et al., 2008; Kondoh and Kamachi, 2010). SOX10 has thus been shown to play a role in specification and differentiation of the melanocyte lineage by regulating the expression of *MITF/Mitf, TRYP2/Dct* (Dopachrome tautomerase) and tyrosinase genes, in synergy with PAX3 or MITF (Bondurand et al., 2000; Potterf et al., 2000; Jiao et al., 2004; Ludwig et al., 2004; Murisier et al., 2007). It is also crucial for the maintenance of pluripotency of migrating enteric progenitors and their differentiation, which correlates with

its regulation of two HD genes: *EDNRB* and *RET*, encoding a seven-transmembrane and a tyrosine-kinase receptor respectively (Lang et al., 2000; Lang and Epstein, 2003; Zhu et al., 2004; Yokoyama et al., 2006b). Finally, SOX10 is essential for the survival and differentiation of glial cells of the peripheral nervous system and for oligodendrocyte development. Its transcriptional targets within these cell lineages include *MPZ* (myelin protein zero, P0), *MBP* (myelin basic protein), *PLP* (proteolipid protein), *GJC2* and *GJB1* (connexin 47 and connexin 32 respectively; (Peirano et al., 2000; Bondurand et al., 2001; Britsch et al., 2001; Stolt et al., 2002; Schlierf et al., 2006)). In the case of connexin 32 (Cx32) activation, SOX10 acts in synergy with the EGR2 transcription factor (Bondurand et al., 2001). Some of these promoters contain multiple SOX10-binding sites, which support either monomeric or cooperative dimeric binding (Peirano et al., 2000; Peirano and Wegner, 2000; Bondurand et al., 2001).

The SOX10 mutations characterized so far are mostly truncating mutations: nonsense or frameshift and two splice mutations, which most often remove all or part of the transactivation domain located in the C-terminal part of the protein, and sometimes the HMG domain (Pingault et al., 1998; Pingault et al., 2010). Interestingly, few cases exhibit chronic intestinal pseudo-obstruction instead of HD. In addition to the WS2 and WS4 classic phenotypes, some patients also present with neurological features: peripheral demyelinating neuropathy, central neuropathy, or both, leading to a syndrome called PCWH (Peripheral demyelinating neuropathy-Central dysmyelinating leukodystrophy-Waardenburg syndrome-Hirschsprung's disease) or PCW (PCWH without HD) (MIM 609136 and (Inoue et al., 2004; Pingault et al., 2010)). These more severe phenotypes mostly result from mutations in the last coding exon and have been proposed to occur when the mutant mRNAs escape the nonsense-mediated mRNA decay (NMD) pathway (Inoue et al., 2004). However, the recent identification of whole *SOX10* gene deletions in PCWH patients can not be explained by this

hypothesis (Bondurand et al., 2007).

The first SOX10 missense mutation, p.Ser135Thr, was identified in a patient presenting with a peculiar phenotype, the so-called mild form of Yemenite syndrome (reminiscent of WS2 or PCW cases; (Bondurand et al., 1999)). *In vitro* functional studies have suggested that this mutant may differentially influence expression of lineage-specific target genes, accounting for the phenotypic differences observed. Indeed, this mutation abolishes DNA binding but maintains transcriptional activation of *RET* and *EDNRB* (and therefore proper enteric development), but not *MITF* (Bondurand et al., 1999; Lang and Epstein, 2003; Yokoyama et al., 2006b; Yokoyama et al., 2006a). Since then, two other missense mutations have been reported, p.Ala157Val and p.Gln174Pro, associated with WS4 and PCW respectively (Morin et al., 2008; Barnett et al., 2009). In the present study, novel SOX10 missense mutations, associated with a variety of phenotypes, ranging from WS2 to WS4 and PCWH, were identified from 11 patients. In addition, the functional effects of all missense mutations described to date and not previously characterized in terms of function were analyzed.

Materials and methods

SOX10 mutation screening:

Informed consent for genetic testing was obtained from patients and/or parents. Genomic DNA was extracted from peripheral blood leukocytes using standard protocols.

Patients A, F, G, and K were screened using dHPLC (primers available upon request). All amplicons showing a difference compared with the controls were then sequenced. The three coding exons of the other patients were analyzed by direct sequencing of the PCR products as previously described (Bondurand et al., 2007). In the absence of a full description of the 5'UTR non-coding exon(s) of *SOX10*, the exon numbering system previously used was conserved, *i.e.*, the non-coding exons are designated exons 1 and 2, the exon with the ATG

codon is designated exon 3, and the exon with the stop codon is designated exon 5. Mutations were named according to international nomenclature based on cDNA numbering with +1 corresponding to the A of the ATG translation initiation codon in the cDNA reference sequence (GenBank NM_006941.3). To confirm their *de novo* occurrence, comparison with the parental DNA, along with verification of sample identity, was conducted through analysis of six microsatellites located on six different chromosomes, using the linkage mapping set (Applied Biosystems, Carlsbad, CA, USA).

Bioinformatics and 3D analysis:

The mutations identified were not described as known polymorphisms in the relevant databases, dbSNP (http://www.ncbi.nlm.nih.gov/snp) or 1000 genomes project (http://browser.1000genomes.org) and all of them are predicted as probably damaging by the functional effects of missense variation prediction software, PolyPhen (http://genetics.bwh.harvard.edu/pph). All mutations were analyzed using Human Splicing Finder v2.4 (Deslet FO, NAR 2004), which runs splice detection software, as well as ESEfinder to verify the absence of significant predicted splice alteration (http://www.umd.be/HSF).

The SOX10 HMG box sequence was analyzed by BLAST search of the RefSeq protein database (http://blast.ncbi.nlm.nih.gov/Blast.cgi). The HMG sequences of other species or other SOX proteins were then aligned using ClustalW software (http://www.ebi.ac.uk/Tools/clustalw2/index.html) and amino acid variability was evaluated using the Variability Protein Server VPS (http://imed.med.ucm.es/PVS/).

Protein data bank files were imported from http://www.pdb.org/pdb/home/home.do (accession codes 3F27 and 1GT0 for SOX17/DNA and SOX2/OCT4/DNA conformation respectively) and models were presented by the Swiss-Pdb Viewer software.

Plasmid constructs:

The pCMV-SOX10Myc, pECE-SOX10, pECE-E189X, pECE-PAX3, pECE-EGR2, pGL3-MITFdel1718, and pGL3-Cx32 vectors have been previously described (Bondurand et al., 2000; Bondurand et al., 2001; Sanchez-Mejias et al., 2010). The P0 and pSOX10-GFP constructs were kindly provided by M. Wegner (Peirano and Wegner, 2000; Rehberg et al., 2002). The padRSVkrox20gHA construct was provided by P. Gilardi-Hebenstreit (Desmazieres et al., 2009). The Ret enhancer region MSC+9.7wt plasmid was kindly provided by A. McCallion (Emison et al., 2010).

All mutations were introduced within the corresponding constructs by site-directed mutagenesis using the QuikChange Site-Directed Mutagenesis Kit (Stratagene, La Jolla, CA, USA). Two different nucleotidic changes are predicted to induce the same p.Met112Ile mutation; of these, the recurrent c.336G>A substitution was chosen for the study. A c.340_341delTGinsGT change was introduced within the pECE-SOX10 vector to create a p.Trp114Val substitution.

Cell culture, transfection, and reporter assays:

HeLa cells were grown in Dulbecco's modified Eagle's medium (DMEM) supplemented with 10% fetal calf serum and transfected using Lipofectamine PLUS reagents (Invitrogen, Carlsbad, CA, USA). Cells were plated on 12-well plates and transfected 1 day later with 0.150 μg of each effector and reporter plasmid for the Cx32 promoter analysis or with 0.175 μg of each effector and reporter plasmid for the MITF promoter study. The total amount of plasmid was kept constant by the addition of empty pECE vector. Twenty-four hours post-transfection, cells were washed twice with PBS, lysed, and the extracts were assayed for luciferase activity using the Luciferase Assay System (Promega, Madison, WI, USA) as described previously (Bondurand et al., 2000; Bondurand et al., 2007). In the case of P0, 1.5 μg of reporter plasmid was used in combination with 0.400 μg of effector, and luciferase activity was measured 72 hours post-transfection. Regarding RET, 0.400 μg of reporter and

effector plasmids were used, and luciferase activity was assayed 48 hours post-transfection (Emison et al., 2010). For competition assays, increasing amounts of mutant SOX10 plasmids, 0.150 µg (1X) or 0.300 µg (2X), were mixed with a fixed amount of wild-type SOX10 (0.150 µg) and the reporter pGL3-Cx32 plasmid (0.150 µg). The DNA per well was kept constant by adding empty pECE vector.

Gel shifts and Western blots:

^{33}P-labeled S1S2, S5 or C/C' probes (0.5 ng) were incubated with proteins as previously described (Peirano et al., 2000). Experiments were carried out with truncated SOX10 versions (amino acids 1–188) bearing the wild-type or mutated sequences (5 µg / reaction or 10 µg / reaction in case of mutants presenting with nucleocytoplasmic relocalization). Double-stranded oligonucleotides containing one or two SOX10-binding sites from the MITF (S5), Cx32 (S1S2) or P0 (C/C') promoter regions were used as probes (for sequences, see (Bondurand et al., 2000; Peirano et al., 2000; Peirano and Wegner, 2000; Bondurand et al., 2001)). In some reactions, a specific competitor (C/C'mut probe) was added in a range of 5- to 10-fold molar excess. In each case, production of SOX10 proteins was assessed by Western blot using 25 µg or 50 µg (in case of mutants presenting with nucleocytoplasmic relocalization) of proteins obtained from nuclear extracts (Fig. 2A).

For analysis of protein stability, HeLa cells were transfected with wild-type or mutant SOX10 constructs and treated 24 hours after transfection with 25 µg/ml cycloheximide for up to 12 hours. Extracts were prepared after various times of treatment, and SOX10 detected by Western blot. Quantification was performed using the GeneTools v3.05 software.

Immunofluorescence:

HeLa, SKMel5 or N2A cells were plated on 24-well plates and transfected 1 day later with 0.400 µg of expression vectors. Twenty-four hours after transfection, cultures were fixed in 4% paraformaldehyde for 10 minutes at RT and immunohistochemistry was performed as

previously described (Bondurand et al., 2007), using the following primary and secondary antibodies: SOX10-N20 (goat; Santa Cruz Biotechnology, INC., Santa Cruz, CA, USA) 1:50; anti-goat Alexa Fluor 546 (Molecular Probes, Eugene, Oregon, USA) 1:200. Cells were counterstained with TO-PRO-3-iodide (Molecular Probes, Eugene, Oregon, USA; 1:1000 in PBS), mounted using Vectashield without 4', 6-Diamidino-2-Phenylindole (DAPI) (Vector Laboratories, Burlingame, CA, USA) and examined with a Zeiss Axioplan 2 confocal microscope. Images were analyzed using the Metaphor software package. Other antibodies used are specified within the legends of supplementary figures.

ResultsIdentification of new SOX10 missense mutations.

Genetic investigations of patients presenting with classical forms of WS2 and WS4, as well as the PCW or PCWH clinical variants, led us to identify 10 new missense mutations in 11 independent cases: p.Arg106Trp, p.Met112Ile (found in three independent families and resulting from two different variations at the nucleotide level: c.336G>A and c.336G>C), p.Asn131His, p.Leu145Pro, p.Lys150Asn and p.Gly321Arg found in the same patient, p.Arg161His, p.Pro175Ala, p.Pro175Leu, and p.Pro175Arg. These findings are summarized in Table 1 along with the corresponding clinical diagnosis. The two missense variations characterized in patient G, p.Lys150Asn and p.Gly321Arg, occurred *de novo*. Whether they are on the same or different alleles could not be assessed. Except for p.Gly321Arg, all of these substitutions were located in exon 3 or 4 (see comment in materials and methods regarding exon numbering) and *in silico* analysis did not predict a major alteration of splicing. The production of a full-length protein with a single amino acid change remains the most likely outcome in all cases.

As for truncating mutations, most missense mutations occurred *de novo*. Only two familial cases were observed, with the mutation segregating in several patients over two generations

(Table 1). A large variety of phenotypes was observed, ranging from classical WS2 or WS4 to severe PCWH. Of particular interest, the p.Met112Ile substitution was associated with WS2 or PCW/PCWH in independent families. The same c.336G>A change occurred twice independently, a situation rarely observed for *SOX10* mutations. Along the same lines, the proline located at position 175 was altered by three distinct changes (patients K, L, and M).

Two other missense mutations were recently published (Morin et al., 2008; Barnett et al., 2009), but their functional consequences were not evaluated. These mutations and their associated phenotypes are also presented in Table 1 (patients H and J).

With the exception of p.Gly321Arg, all of these variations were located within one of the main functional domains of the SOX10 protein, *i.e.*, the HMG DNA binding domain (Fig. 1). ClustalW alignment of the SOX10 HMG box showed that concerned amino acids are fully conserved across evolution (18 species analyzed, data not shown). Moreover, alignment and a variability plot of all human SOX family members showed that these mutations modify relatively conserved amino acids within the HMG box: four out of the nine amino acids concerned are fully conserved among all of the SOX members analyzed, SRY included. An alignment between SOX10 and one member of each SOX subgroup is presented in Fig.1. Interestingly, five of the mutations are located in import or export localization signals.

DNA binding and transactivation capacities of the mutant proteins.

To analyze the monomeric and/or dimeric binding capacities of the mutants, electrophoretic mobility shift assays (EMSA) were performed using two different probes: “S5”, the SOX10 monomeric binding site from the *MITF* promoter, and “S1S2”, the SOX10 dimeric binding sites from the Cx32 (*GJB1*) promoter. The previously characterized p.Glu189X mutant was included in all experiments as a positive control. p.Arg106Trp, p.Leu145Pro, p.Lys150Asn, and p.Ala157Val mutants completely lost their DNA binding capacities for both probes (Fig. 2B and C, lanes 3, 6, 7, 8). Other mutants tested retained partial DNA binding capacities for

one or both probes, compared with the control (Fig. 2B and C, compare line 2 to lines 5, 9, 10, 11, 12, 13). Interestingly, the p.Met112Ile mutant seemed to present with an increased monomer-binding capacity on the "S1S2" probe (Fig. 2C, lane 4). Quantification of the dimer over monomer ratio confirmed these observations. Indeed, a ratio of 2.4 ± 0.4 and 1.8 ± 0.2 was observed for the p.Glu189X and p.Met112Ile mutants respectively. To confirm this latter observation, binding of this mutant to another well-defined dimeric binding probe, the C/C' probe of the *MPZ* promoter, was tested. Site C/C' consists of two non-consensus sites with distinct spacing and orientation (Peirano and Wegner, 2000) that favors cooperative binding of two molecules. Its use also suggested that p.Met112Ile presented with increased monomeric binding (Fig. 2D, compare lines 1 and 4). In this case, we observed a dimer over monomer ratio of 5 and 3 respectively. Interestingly, Peirano et al. reported that a mutation of site C' (C'mut probe) resulted in monomeric instead of dimeric binding (Peirano and Wegner, 2000), suggesting that this probe still presented with high affinity to SOX10 monomers. Therefore, the ability of p.Met112Ile to bind was compared to the control in the presence of the C/C' probe upon C'mut competition. This competition reduced binding of the SOX10 mutant more efficiently than that of the wild-type SOX10 (Fig. 2D, compare lines 4-5 to 2-3), thus confirming increased p.Met112Ile mutant binding as a monomer.

Next, the transactivation potential of each of these mutants was analyzed *in vitro*. We chose to compare their transactivation capacities on *MITF*, Cx32, and *RET* promoters/enhancers, alone or in synergy with their partners, thus testing whether phenotype differences observed among patients could be related to the differential regulation of target genes. We used *MITF* and *Cx32* reporter constructs containing promoter regions of each of these genes. Transactivation depends on SOX10 and PAX3 in case of *MITF* and SOX10 and EGR2 in case of Cx32 (Bondurand et al., 2000; Bondurand et al., 2001). As far as RET is concerned, we analyzed the transactivation capacities of the SOX10 mutants on the recently identified SOX10-

responsive enhancer located within the *RET* intron 1 ((Emison, et al., 2010) and Fig.3C). p.Arg106Trp, p.Leu145Pro, p.Lys150Asn, and p.Ala157Val were unable to transactivate the reporter constructs alone or in synergy with their respective cofactors (Fig. 3A, B, and C). Other mutants retained partial activity. Indeed, p.Gln174Pro and the 3 p.Pro175 mutants maintained partial or complete activity of the *RET* enhancer and the *MITF* promoter, alone or in synergy with PAX3. However, they failed to transactivate the Cx32 promoter, alone or in synergy with EGR2. The p.Arg161His mutant exerted the opposite effects. This mutant was able to activate the Cx32 promoter in a manner similar to that of the wild-type protein, but its activity on *MITF* and *RET* was null or much reduced. By contrast, only RET enhancer activity was reduced upon p.Asn131His mutant co-transfection. Finally, the transactivation capacities of the p.Met112Ile mutant were normal for all three reporter genes tested. Based on the results obtained regarding this particular mutant in EMSA experiments using the MPZ probe C/C' (see Fig. 2C), similar studies were performed using the MPZ promoter as a reporter gene. In agreement with its dimeric binding defects, the p.Met112Ile mutant presented with reduced transactivation capability on this promoter (Fig. 3D).

As mentioned above, patient G presented with two missense variations, both of which occurred *de novo*. The functional relevance of the p.Gly321Arg variation, which is located distal to the HMG domain and outside any known functional domain, was tested alone and in combination with the p.Lys150Asn mutation. p.Gly321Arg maintained full transactivation activity on *MITF* and *Cx32* promoters (Supp.Fig.S1). By contrast, the double mutant presented with null transactivation capacity. These results strongly argue in favor of the p.Lys150Asn mutation as the primary cause of the disease. The p.Gly321Arg variation was therefore not included in further studies.

Previous papers have suggested that the presence or absence of the neurological phenotypes that characterize PCWH syndrome could be related to a nonsense-mediated mRNA decay

(NMD) process (Inoue et al., 2004). Most identified mutations lead to truncated proteins with dominant-negative effects *in vitro*. However, truncating mutations located in the first coding exons (exons 3 and 4) activate the NMD mRNA surveillance pathway and lead to an absence of the mutant protein *in vivo* (haploinsufficiency), resulting in the classic form of WS4. On the other hand, truncating mutations located in the last coding exon (exon 5) escape nonsense mRNA decay and lead to translation of a mutant SOX10 protein that interferes with the function of the normal SOX10 allele. This dominant-negative effect leads to the more severe PCWH phenotype. The fact that missense mutations are not subject to NMD argues in favor of other mechanisms at the origin of the phenotype variability we observed here. To test the ability of each SOX10 mutant protein to interfere with wild-type SOX10 function, we carried out competition assays by co-transfecting mutant and wild-type SOX10-expressing vectors together with the Cx32 reporter plasmid. As previously described, the p.Glu189X mutant decreased the transcriptional activity of the wild-type protein in a dose-dependent manner (Fig. 3E, (Inoue et al., 2004; Sanchez-Mejias et al., 2010)). However, none of the missense mutants tested in the present study presented with such an effect (Fig. 3E). According to our experimental results on this specific reporter gene, dominant-negative activity does not appear to correlate with PCWH phenotype observed in several patients.

Subcellular localization of mutant proteins.

We next compared the localization of wild-type and mutant proteins in HeLa cells (Fig. 4), as well as N2A, and SKMel5 cells (data not shown). In all cell types analyzed, wild-type SOX10 protein was distributed in a diffuse pattern throughout the nucleoplasm (Fig. 4, panels A1-A4 and Fig.5A). p.Met112Ile, p.Asn131His, p.Gln174Pro, and the three p.Pro175 SOX10 mutant proteins retained nuclear localization (Fig. 4, panels C1-4, D1-4, I1-4, J1 to L4). By contrast, the p.Arg106Trp, p.Leu145Pro, p.Lys150Asn, p.Ala157Val, and p.Arg161His proteins were partially redistributed in the cytoplasm (Fig. 4, panels B1-4, E1-4, F1-4, G1-4, H1-4). This

redistribution occurred in 80% to 92% of cells transfected cells except for p.Arg161His (37%) (Fig.5A). Partial cytoplasmic redistribution could therefore be at the origin of the deleterious effects of about half of the mutations identified.

Surprisingly, seven of the mutations induced a striking nuclear redistribution of SOX10 proteins into punctate structures or inclusions that will be called foci within the remaining of the paper. This event, which was not observed upon wild-type construct transfection, occurred irrespective of nuclear or nucleo-cytoplasmic localization. The number of foci ranged from one to greater than 20 per nucleus. Foci observed with the three p.Pro175 mutants were small (from 0.70 to 1.1 μm) and detected in 20% of the cells (Fig. 4 J4, K4, L4 and Fig. 5B). Those observed with the p.Leu145Pro, p.Lys150Asn, p.Ala157Val, and p.Gln174Pro mutants were larger (ranging from 1.3 to 6 μm) and detected in 26–70% of the transfected cells (Fig. 4 E4, F4, G4, I4, and Fig. 5B). Interestingly, the number and size of foci changed over time. They were observed as early as 3 hours post-transfection and increased in size for up to 48 hours while decreasing in number (data not shown), arguing in favor of foci fusion over time.

Several subnuclear compartments that are enriched in specific proteins have been described in eukaryotic cells (Matera, 1999; Matera et al., 2009; Carmo-Fonseca et al., 2010). In an attempt to identify the nature of these foci, co-immunolabeling was performed with various markers, such as SC35 for nuclear speckles, PML for PML bodies, and ubiquitin for nuclear aggresomes (Fu and Maniatis, 1990; Dyck et al., 1994; Borden, 2002). None of these markers co-localized with the SOX10 mutant proteins within the punctate foci. Supp.Fig.S2 shows results obtained for p.Leu145Pro, but similar observations were made for all mutants analyzed. The exact nature of these foci remains to be determined.

Molecular consequences of subnuclear redistribution

Finally, we focused on the molecular and cellular events that could be responsible for foci formation or that could be triggered by foci formation.

Since all *SOX10* mutations are dominant, their pathological effects could be due to a gain of function. The competition assay we carried out (Fig. 3E) seems to argue against a dominant-negative effect. Another possibility is that SOX10 missense mutants recruit wild-type SOX10 or interacting partners to the subnuclear foci and thereby exert their deleterious effects. To test this hypothesis, we compared the distribution of a myc-tagged version of wild-type SOX10 upon co-transfection with mutants fused to green fluorescent protein (GFP) or GFP-fused wild-type SOX10. Cells co-transfected with plasmids containing GFP and myc-tagged versions of wild-type SOX10 exhibited uniform nucleoplasmic staining (Supp.Fig.S3, Top panels). Upon wild-type and mutant co-transfection, areas stained by GFP (mutant) and myc (wild-type) were redistributed within foci, indicating that SOX10 mutants could recruit wild-type protein to the punctate foci. Supp.Fig.S3A, bottom panels shows results obtained for p.Leu145Pro, but similar observations were made for p.Ala157Val, p.Gln174Pro, and p.Pro175Arg mutants . On the other hand, co-transfection seemed to decrease the percentage of cells presenting with the punctate pattern, suggesting that wild-type SOX10 expression could partially protect against mutant protein redistribution. In the case of p.Leu145Pro, the percentage of transfected cells containing foci dropped from 34,9 ± 0,3% to 8,1 ± 0,1%. Similar decreases were observed for all mutants analyzed (data not shown).

We next tested whether expression of SOX10 mutants also resulted in redistribution of cofactors. To this end, we co-transfected wild-type or mutant versions of SOX10 with expression vectors containing PAX3 or EGR2 cDNAs. GFP-tagged SOX10 constructs were used to avoid cross-reactions between antibodies. Diffuse nuclear staining was observed for both cofactors, irrespective of the SOX10 construct co-transfected, suggesting that neither of the two cofactors were redistributed within the foci (Supp.Fig.S3B and data not shown).

Interestingly, the mutations leading to nuclear foci formation were all located within the distal half of the HMG domain (Fig. 6A). This primary structure observation led us to determine the

spatial location of the mutant amino acids in 3D reconstructions. As the HMG domain of SOX proteins is highly conserved, we used reconstructions of the closest factors for which structures had been determined by crystallography: SOX17 (67% identity to the SOX10 HMG, 84% similarity, Fig. 6B) and SOX2 (63% identity, 84% similarity) (Remenyi et al., 2003; Palasingam et al., 2009). This led to the interesting observation that several mutations leading to foci accumulation were located either close to or directly surrounding the hydrophobic core that maintains the HMG structural organization (p.Leu145Pro, p.Lys150Asn, p.Ala157Val, Fig. 8B2). By contrast, missense mutations located at the interface with the DNA did not lead to foci formation (p.Arg106Trp, p.Met112Ile, p.Asn131His, Fig. 8B2). The p.Gln174Pro and the three p.Pro175 mutations were in the C-tail of the HMG domain, which is distal to helix 3 and makes contacts both with the N-tail and the DNA minor groove. Their possible functions are more difficult to predict from 3D models (see Fig. 6B3 and Discussion).

These observations led us to propose two hypotheses to explain foci formation: i) an alteration of an unknown functional domain in the distal half of the HMG domain primary structure; or ii) formation of an abnormal tertiary structure resulting in incorrect folding of the protein. To gain insight into these possibilities, we decided to mutate a codon encoding an amino acid that was part of the hydrophobic core but was located within helix 1 of the HMG domain (proximal half of the HMG domain primary structure; p.Trp114Val; see Fig. 6A and B4). Reminiscent of the effect of mutations surrounding the hydrophobic core, the p.Trp114Val mutant was partially redistributed within large foci (Fig. 6C) and was not able to transactivate *MITF* or *Cx32* promoters, either alone or in synergy with SOX10 cofactors (Fig. 6D). These results indicated that the location of the mutation within the proximal or distal half of the HMG domain was not responsible for foci formation and instead suggested that the foci are induced by alteration of the mutant tertiary structure, possibly resulting in sequestration of

malfolded proteins within these foci. To test whether these observations could be related to protein instability, we compared the wild-type and p.Leu145Pro, p.Lys150Asn, p.Ala157Val proteins half life in transfected cycloheximide treated cells and found no significant differences (Fig. 6E).

Discussion

In addition to our first description of a SOX10 missense mutation in the so-called mild form of Yemenite syndrome, we here report 10 new missense mutations in 11 patients presenting with WS2, WS4, or PCW/PCWH ((Bondurand et al., 1999) and the present study). Two missense mutations were also recently published by other groups (Morin et al., 2008; Barnett et al., 2009), but their functional relevance was not tested. In this report, the effects of all of these functionally uncharacterized mutations on SOX10 characteristics and functions are described. Table 2 summarizes the results obtained and highlights the deleterious effects of the identified mutations, supporting arguments for their pathogenicity.

With the exception of two mutations, p.Gly321Arg, which is probably not the major cause of the disease in the patient (see Table 1 and supplementary data) and p.Val92Leu (which we previously characterized as non-pathogenic; (Bondurand et al., 2007)), all SOX10 missense mutations identified so far are localized in the HMG domain. As a result, some mutants present with partial cytoplasmic and/or subnuclear redistribution, and some lose their DNA binding and transactivation capacities for different tissue-specific target genes. The p.Met112Ile and p.Asn131His mutants were the sole mutants with subtle anomalies. The others presented with one or several gross defects (see Table 2). However, it is sometimes difficult to determine the primary origin of pathogenicity. Several reports have suggested that subcellular localization of SOX factors is finely regulated and essential for their activity (Rehberg et al., 2002; Lefebvre et al., 2007; Malki et al., 2010). Cytoplasmic redistribution

has been linked to SOX-associated pathologies. While some SRY sex-reversing mutations alter both DNA binding and nuclear transport, others affect only nuclear import, suggesting that the latter is the cause of the observed phenotype (Argentaro et al., 2003; Harley et al., 2003; Malki et al., 2010). The partial cytoplasmic redistribution of p.Arg106Trp, p.Leu145Pro, p.Lys150Asn, p.Ala157Val, and p.Arg161His could therefore be considered as the primary defect, despite the null or partial DNA binding and transactivation capacities of these mutants. Interestingly, cytoplasmic redistribution was observed irrespective of the location of the mutations within or outside the NLSs or NES. This was unexpected but may be explained by an indirect effect. Indeed, an abnormal protein configuration induced by a missense mutation distant from any NLS/NES was previously reported in the closely related SOX9 transcription factor, and this mutation resulted in a defective NLS function (Preiss et al., 2001; Argentaro et al., 2003).

As for SOX10, nonsense/truncating mutations identified in SOX9 and in another SOX family member, SRY, are distributed throughout the coding sequence, while missense mutations are mainly (even if not only) located in the HMG domain (reviewed in (Harley et al., 2003)). For almost all of the amino acids affected by SOX10 missense mutations, there are equivalent mutated amino acids in SRY and/or SOX9. Of particular interest the p.Pro131Arg mutation of SRY (Lundberg et al., 1997) and the p.Pro176Leu mutation of SOX9 (Michel-Calemard et al., 2004) are the exact equivalents of the SOX10 mutations p.Pro175Arg and p.Arg175Leu described here. This proline may therefore be a recurrent mutation site in SOX factors. The SOX9 p.Pro176Leu mutation was found in a fetus presenting with sex reversal and acampomelic campomelic dysplasia (ACD) (Michel-Calemard et al., 2004). In contrast to campomelic dysplasia, ACD was suggested to result from reduced, but not fully abolished, SOX9 function (Staffler et al., 2010). These observations are consistent with the functional consequences of the SOX10 p.Pro175Leu mutation reported here. A SOX9 mutation

p.Met113Val, located on the equivalent of the SOX10 Met112, is also associated with ACD. This mutant was shown to be located essentially within the nucleus, although a faint cytoplasmic staining was noted. DNA binding and reporter gene activation were reduced (Staffler et al., 2010) and, similar to our observations, modification of the monomeric versus dimeric binding ratio was apparent on the figure. Amino acids affected by missense mutations in various SOX members thus seem to present with similar functional effects. However, their link to specific phenotypes is not clear. In our case, p.Pro175Leu and p.Met112Ile mutations were associated with different phenotypes (PCW vs. WS2, PCWH or PCW, respectively).

As opposed to truncating mutations, which are subject to the NMD pathway, missense mutations located in exons 3 and 4 can lead to PCW/PCWH. Searching for other mechanisms responsible for phenotype variability was therefore of prime interest. The p.Ser135Thr mutation was the only missense mutation described so far in terms of functional effects. Several studies have suggested that this mutant may differentially influence tissue-specific gene expression, accounting for the phenotypic differences observed (Lang and Epstein, 2003; Yokoyama et al., 2006b; Yokoyama et al., 2006a). In an attempt to identify molecular mechanisms underlying the phenotype variability observed in our patients, we performed similar experiments by testing the transactivation capacities of mutant proteins on melanocytic (*MITF*), enteric (*RET*) and glial (*Cx32*) gene expression. No correlation between tissue-specific promoter activation and the phenotypes observed was evident. Indeed, despite the fact that six of the mutants studied maintained complete or partial activity of the *MITF* promoter, all patients presented with pigmentation defects. Along the same lines, the p.Met112Ile mutation did not alter the capacity of SOX10 to activate the Cx32 promoter; however, two out of the three patients harboring this mutation presented with severe neurological defects (see Tables 1 and 2). No correlation between RET activation and ENS defects was apparent either. The differential tissue-specific target gene transactivation

observed *in vitro* does not seem to be the main basis for phenotype variability observed here. We finally considered the possibility that SOX10 mutations associated with severe phenotypes could exert dominant-negative effects on wild-type SOX10. Within the limits of our experimental assay, competition assays did not favor this hypothesis. The molecular origin of phenotype variability thus remains to be established.

One of the most striking findings of our study was the observation that seven of the mutants analyzed presented with altered subnuclear distribution within structures that we called foci. The nuclei of eukaryotes contain various structures that have been characterized morphologically and are collectively referred to as “nuclear bodies”. The wide variety of components that are concentrated within these structures makes them a likely interface for multiple cellular processes, including transcription, RNA processing, transport, protein modification, apoptosis, and cell cycle control (Matera, 1999; Matera et al., 2009). SOX factors were previously found to be associated with some of these structures upon post-translational modifications such as phosphorylation, acetylation and sumoylation (Sachdev et al., 2001; Thevenet et al., 2004; Fernandez-Lloris et al., 2006; Lefebvre et al., 2007). In context of the latter, it was previously shown that SOX6 and Sumo 2 co-expression results in the appearance of SOX6 in a punctate pattern that co-localizes with PML but which is partially abolished by alteration of SOX6 sumoylation sites (Fernandez-Lloris et al., 2006). In our case, preliminary results indicated that co-transfection with Sumo 1, 2, or 3, or alteration of SOX10 sumoylation sites did not appear to modify the punctate relocation. SRY and SOX6 have also been associated with splicing factors such as SC35 (Ohe et al., 2002). In our study, none of the SOX10 mutants co-localized with this marker, suggesting that the foci observed were not nuclear speckles. However, previous results suggested that SOX9 interacts with another nuclear RNA binding protein ($p54^{nrb}$) within paraspeckels, an interaction that links SOX9-dependent transcription to target gene mRNA maturation during chondrogenesis (Hata

et al., 2008). Whether similar events could explain our observations should be tested in the near future.

Whether these foci are the main cause of pathogenic effects or a consequence of them is not clear, but such subnuclear relocalization has not been extensively described in functional studies of other SOX gene mutations identified in patients. To our knowledge, only the polyalanine expansion mutations identified in *SOX3* were reported to generate cellular aggregates (Wong et al., 2007). The type of mutations we identified is very different and our results argue against similar mechanisms at the origin of accumulations. Outside of the SOX family, mutations in other transcription factors have been shown to modify subnuclear localization. An R288P mutation within the DNA binding domain of Maf, which had been shown to cause cataracts, eliminated the transcriptional activity of this transcription factor without altering DNA binding. This mutant was enriched in nuclear foci of unknown origin (Rajaram and Kerppola, 2004) and recruited SOX as well as other interaction partners within these structures, providing a potential explanation for the dominant disease phenotype. In our case, foci observations were not directly linked to loss of DNA binding or transactivation capacities. We also determined whether cofactors could be recruited within nuclear foci, but none of the results argued in favor of this hypothesis. Based on 3D modeling, we finally considered the possibility that some of these “punctate” mutants, namely p.Leu145Pro, p.Lys150Asn, and p.Ala157Val, disrupt the tertiary structure of the HMG domain. Interestingly, a similar situation has been described for homeodomain transcription factors. The homeodomain is composed of three α-helices folded around a hydrophobic core that maintains the 3D conformation. Missense mutations have been mainly localized to DNA contact sites and within the hydrophobic core, resulting in either altered DNA binding or destructuration as the main cause of the disease phenotypes (Chi, 2005). In our case, all three mutations may affect formation of the hydrophobic core without obviously affecting protein

stability, resulting in sequestration of malfolded proteins within foci.

Interpretation is more difficult with the p.Gln174 and p.Arg175 mutations. Gln174 is specific to the SoxE subgroup proteins and thus is not found in the SOX2 and SOX17 HMG domains we used as models. In addition, these two amino acids are located close to the terminal end of the domain used for crystallography. They may not, therefore, be fully representative of the structure in the whole SOX proteins. This HMG C-tail, the structure of which is one of the most variable among HMG domains, has been shown to change conformation upon DNA binding (Palasingam et al., 2009) to make a secondary hydrophobic core and establish several contacts with the minor groove (Murphy et al., 2001). As a result, these mutations may affect DNA binding or 3D structure. Other hypotheses could also explain their pathogenicity. They all create or remove a proline in the C-tail, possibly leading to an abnormal position of the whole carboxy end of the protein. They could also affect binding to cofactors as the distal part of the HMG domain is involved in contacts with cofactors (Wissmuller et al., 2006). However, our experimental results do not favor this hypothesis, as two of the p.175 mutants retained synergistic activity with PAX3.

Very few SOX10 missense mutations have been characterized so far. In this study, we show that such mutations are not as rare as previously described. As opposed to the hypotheses made in the context of the p.Ser135Thr mutant study (Bondurand et al., 1999; Lang and Epstein, 2003), in the present study, we found no argument for a link between the activation of tissue-specific promoters/enhancers *in vitro* and the resulting phenotype. However, the observation that the p.Met112Ile mutation is recurrent (a very rare situation in SOX10) and leads to different phenotypes opens the possibility that the genetic background is influential, as is often suggested for neurocristopathies, and Hirschsprung's disease in particular (Gabriel et al., 2002; Chakravarti, 2003; McCallion et al., 2003; Amiel et al., 2008). Finally, the redistribution of several missense SOX mutant proteins into nuclear foci is intriguing. The

characterization of their molecular nature may help to clarify whether they are a cause or a consequence of mutation-related pathogenicity, and furthermore, will provide opportunities for enhanced understanding of the function and mode of action of SOX10 and possibly other SOX factors.

Acknowledgments:

This work was supported by the Institut National de la Santé et de la Recherche Médicale (INSERM) and Agence Nationale de la Recherche (ANR-JCJC).

We would like to thank Natacha Martin and Bruno Costes for sequencing, Xavier Decrouy for confocal microscopy. Drs JL. Alessandri (Saint-Denis, La Reunion, France), J. Amiel (Paris, France), A. Colley (Liverpool, Australia), A. Fryer (Liverpool, UK), B. Gilbert (Poitiers, France), M. Holder (Lille, France), A. Jacquette (Paris, France), S. Manouvrier (Lille, France), L. Pierre-Louis (Fort-de-France, France), P. Uldall (Copenhagen, Denmark) for providing patient data.

References

Amiel J, Sproat-Emison E, Garcia-Barcelo M, Lantieri F, Burzynski G, Borrego S, Pelet A, Arnold S, Miao X, Griseri P and others. 2008. Hirschsprung disease, associated syndromes and genetics: a review. J Med Genet 45:1-14.

Argentaro A, Sim H, Kelly S, Preiss S, Clayton A, Jans DA, Harley VR. 2003. A SOX9 defect of calmodulin-dependent nuclear import in campomelic dysplasia/autosomal sex reversal. J Biol Chem 278:33839-47.

Barnett CP, Mendoza-Londono R, Blaser S, Gillis J, Dupuis L, Levin AV, Chiang PW, Spector E, Reardon W. 2009. Aplasia of cochlear nerves and olfactory bulbs in association with SOX10 mutation. Am J Med Genet A 149A:431-6.

Bernard P, Sim H, Knower K, Vilain E, Harley V. 2008. Human SRY inhibits beta-catenin-mediated transcription. Int J Biochem Cell Biol 40:2889-900.

Bolande RP. 1974. The neurocristopathies: a unifying concept of disease arising in neural crest maldevelopment. Hum Pathol 5:409-429.

Bondurand N, Dastot-Le Moal F, Stanchina L, Collot N, Baral V, Marlin S, Attie-Bitach T, Giurgea I, Skopinski L, Reardon W and others. 2007. Deletions at the SOX10 gene locus cause Waardenburg syndrome types 2 and 4. Am J Hum Genet 81:1169-85.

Bondurand N, Girard M, Pingault V, Lemort N, Dubourg O, Goossens M. 2001. Human Connexin 32, a gap junction protein altered in the X-linked form of Charcot-Marie-

Tooth disease, is directly regulated by the transcription factor SOX10. Hum Mol Genet 10:2783-95.

Bondurand N, Kuhlbrodt K, Pingault V, Enderich J, Sajus M, Tommerup N, Warburg M, Hennekam RC, Read AP, Wegner M and others. 1999. A molecular analysis of the yemenite deaf-blind hypopigmentation syndrome: SOX10 dysfunction causes different neurocristopathies. Hum Mol Genet 8:1785-9.

Bondurand N, Pingault V, Goerich DE, Lemort N, Sock E, Le Caignec C, Wegner M, Goossens M. 2000. Interaction among SOX10, PAX3 and MITF, three genes altered in Waardenburg syndrome. Hum Mol Genet 9:1907-17.

Borden KL. 2002. Pondering the promyelocytic leukemia protein (PML) puzzle: possible functions for PML nuclear bodies. Mol Cell Biol 22:5259-69.

Britsch S, Goerich DE, Riethmacher D, Peirano RI, Rossner M, Nave KA, Birchmeier C, Wegner M. 2001. The transcription factor Sox10 is a key regulator of peripheral glial development. Genes Dev 15:66-78.

Carmo-Fonseca M, Berciano MT, Lafarga M. 2010. Orphan nuclear bodies. Cold Spring Harb Perspect Biol 2:a000703.

Chakravarti A, McCallion, A.S., and Lyonnet, S. 2003. Hirschsprung disease. The metabolic and molecular bases of inherited disease. New york: Scriver, Beaudet.

Chi YI. 2005. Homeodomain revisited: a lesson from disease-causing mutations. Hum Genet 116:433-44.

Desmazieres A, Charnay P, Gilardi-Hebenstreit P. 2009. Krox20 controls the transcription of its various targets in the developing hindbrain according to multiple modes. J Biol Chem 284:10831-40.

Dyck JA, Maul GG, Miller WH, Jr., Chen JD, Kakizuka A, Evans RM. 1994. A novel macromolecular structure is a target of the promyelocyte-retinoic acid receptor oncoprotein. Cell 76:333-43.

Emison ES, Garcia-Barcelo M, Grice EA, Lantieri F, Amiel J, Burzynski G, Fernandez RM, Hao L, Kashuk C, West K and others. 2010. Differential contributions of rare and common, coding and noncoding Ret mutations to multifactorial Hirschsprung disease liability. Am J Hum Genet 87:60-74.

Fernandez-Lloris R, Osses N, Jaffray E, Shen LN, Vaughan OA, Girwood D, Bartrons R, Rosa JL, Hay RT, Ventura F. 2006. Repression of SOX6 transcriptional activity by SUMO modification. FEBS Lett 580:1215-21.

Foster JW, Dominguez-Steglich MA, Guioli S, Kowk G, Weller PA, Stevanovic M, Weissenbach J, Mansour S, Young ID, Goodfellow PN and others. 1994. Campomelic dysplasia and autosomal sex reversal caused by mutations in an SRY-related gene. Nature 372:525-30.

Fu XD, Maniatis T. 1990. Factor required for mammalian spliceosome assembly is localized to discrete regions in the nucleus. Nature 343:437-41.

Gabriel SB, Salomon R, Pelet A, Angrist M, Amiel J, Fornage M, Attie-Bitach T, Olson JM, Hofstra R, Buys C and others. 2002. Segregation at three loci explains familial and population risk in Hirschsprung disease. Nat Genet 31:89-93.

Guth SI, Wegner M. 2008. Having it both ways: Sox protein function between conservation and innovation. Cell Mol Life Sci 65:3000-18.

Harley VR, Layfield S, Mitchell CL, Forwood JK, John AP, Briggs LJ, McDowall SG, Jans DA. 2003. Defective importin beta recognition and nuclear import of the sex-determining factor SRY are associated with XY sex-reversing mutations. Proc Natl Acad Sci U S A 100:7045-50.

Hata K, Nishimura R, Muramatsu S, Matsuda A, Matsubara T, Amano K, Ikeda F, Harley VR, Yoneda T. 2008. Paraspeckle protein p54nrb links Sox9-mediated transcription with RNA processing during chondrogenesis in mice. J Clin Invest 118:3098-108.

Hong CS, Saint-Jeannet JP. 2005. Sox proteins and neural crest development. Semin Cell Dev Biol 16:694-703.

Inoue K, Khajavi M, Ohyama T, Hirabayashi S, Wilson J, Reggin JD, Mancias P, Butler IJ, Wilkinson MF, Wegner M and others. 2004. Molecular mechanism for distinct neurological phenotypes conveyed by allelic truncating mutations. Nat Genet 36:361-9.

Jiao Z, Mollaaghababa R, Pavan WJ, Antonellis A, Green ED, Hornyak TJ. 2004. Direct interaction of Sox10 with the promoter of murine Dopachrome Tautomerase (Dct) and synergistic activation of Dct expression with Mitf. Pigment Cell Res 17:352-62.

Kamachi Y, Uchikawa M, Kondoh H. 2000. Pairing SOX off: with partners in the regulation of embryonic development. Trends Genet 16:182-7.

Kelsh RN. 2006. Sorting out Sox10 functions in neural crest development. Bioessays 28:788-98.

Kondoh H, Kamachi Y. 2010. SOX-partner code for cell specification: Regulatory target selection and underlying molecular mechanisms. Int J Biochem Cell Biol 42:391-9.

Lang D, Chen F, Milewski R, Li J, Lu MM, Epstein JA. 2000. Pax3 is required for enteric ganglia formation and functions with Sox10 to modulate expression of c-ret. J Clin Invest 106:963-71.

Lang D, Epstein JA. 2003. Sox10 and Pax3 physically interact to mediate activation of a conserved c-RET enhancer. Hum Mol Genet 12:937-45.

Le Douarin NM, Kalcheim C. 1999. The neural crest. Cambridge: Cambridge University press.

Lefebvre V, Dumitriu B, Penzo-Mendez A, Han Y, Pallavi B. 2007. Control of cell fate and differentiation by Sry-related high-mobility-group box (Sox) transcription factors. Int J Biochem Cell Biol 39:2195-214.

Li B, Phillips NB, Jancso-Radek A, Ittah V, Singh R, Jones DN, Haas E, Weiss MA. 2006. SRY-directed DNA bending and human sex reversal: reassessment of a clinical mutation uncovers a global coupling between the HMG box and its tail. J Mol Biol 360:310-28.

Ludwig A, Rehberg S, Wegner M. 2004. Melanocyte-specific expression of dopachrome tautomerase is dependent on synergistic gene activation by the Sox10 and Mitf transcription factors. FEBS Lett 556:236-44.

Lundberg Y, Ritzén M, Harlin J, Wedell A. 1997. Novel Missense mutation (P131R) in the HMG box of SRY in XY sex reversal. Hum Mutat *Mutation Note #8*:Online.

Malki S, Boizet-Bonhoure B, Poulat F. 2010. Shuttling of SOX proteins. Int J Biochem Cell Biol 42:411-6.

Matera AG. 1999. Nuclear bodies: multifaceted subdomains of the interchromatin space. Trends Cell Biol 9:302-9.

Matera AG, Izaguire-Sierra M, Praveen K, Rajendra TK. 2009. Nuclear bodies: random aggregates of sticky proteins or crucibles of macromolecular assembly? Dev Cell 17:639-47.

McCallion AS, Emison ES, Kashuk CS, Bush RT, Kenton M, Carrasquillo MM, Jones KW, Kennedy GC, Portnoy ME, Green ED and others. 2003. Genomic variation in multigenic traits: Hirschsprung disease. Cold Spring Harb Symp Quant Biol 68:373-81.

Michel-Calemard L, Lesca G, Morel Y, Boggio D, Plauchu H, Attia-Sobol J. 2004. Campomelic acampomelic dysplasia presenting with increased nuchal translucency in the first trimester. Prenat Diagn 24:519-23.

Mollaaghababa R, Pavan WJ. 2003. The importance of having your SOX on: role of SOX10 in the development of neural crest-derived melanocytes and glia. Oncogene 22:3024-34.

Morin M, Vinuela A, Rivera T, Villamar M, Moreno-Pelayo MA, Moreno F, del Castillo I. 2008. A de novo missense mutation in the gene encoding the SOX10 transcription factor in a Spanish sporadic case of Waardenburg syndrome type IV. Am J Med Genet A 146A:1032-7.

Murisier F, Guichard S, Beermann F. 2007. The tyrosinase enhancer is activated by Sox10 and Mitf in mouse melanocytes. Pigment Cell Res 20:173-84.

Murphy EC, Zhurkin VB, Louis JM, Cornilescu G, Clore GM. 2001. Structural basis for SRY-dependent 46-X,Y sex reversal: modulation of DNA bending by a naturally occurring point mutation. J Mol Biol 312:481-99.

Ohe K, Lalli E, Sassone-Corsi P. 2002. A direct role of SRY and SOX proteins in pre-mRNA splicing. Proc Natl Acad Sci U S A 99:1146-51.

Palasingam P, Jauch R, Ng CK, Kolatkar PR. 2009. The structure of Sox17 bound to DNA reveals a conserved bending topology but selective protein interaction platforms. J Mol Biol 388:619-30.

Peirano RI, Goerich DE, Riethmacher D, Wegner M. 2000. Protein zero gene expression is regulated by the glial transcription factor Sox10. Mol Cell Biol 20:3198-209.

Peirano RI, Wegner M. 2000. The glial transcription factor Sox10 binds to DNA both as monomer and dimer with different functional consequences. Nucleic Acids Res 28:3047-55.

Pingault V, Bondurand N, Kuhlbrodt K, Goerich DE, Prehu MO, Puliti A, Herbarth B, Hermans-Borgmeyer I, Legius E, Matthijs G and others. 1998. SOX10 mutations in patients with Waardenburg-Hirschsprung disease. Nat Genet 18:171-3.

Pingault V, Ente D, Dastot-Le Moal F, Goossens M, Marlin S, Bondurand N. 2010. Review and update of mutations causing Waardenburg syndrome. Hum Mutat 31:391-406.

Potterf SB, Furumura M, Dunn KJ, Arnheiter H, Pavan WJ. 2000. Transcription factor hierarchy in Waardenburg syndrome: regulation of MITF expression by SOX10 and PAX3. Hum Genet 107:1-6.

Poulat F, Girard F, Chevron MP, Goze C, Rebillard X, Calas B, Lamb N, Berta P. 1995. Nuclear localization of the testis determining gene product SRY. J Cell Biol 128:737-48.

Preiss S, Argentaro A, Clayton A, John A, Jans DA, Ogata T, Nagai T, Barroso I, Schafer AJ, Harley VR. 2001. Compound effects of point mutations causing campomelic dysplasia/autosomal sex reversal upon SOX9 structure, nuclear transport, DNA binding, and transcriptional activation. J Biol Chem 276:27864-72.

Rajaram N, Kerppola TK. 2004. Synergistic transcription activation by Maf and Sox and their subnuclear localization are disrupted by a mutation in Maf that causes cataract. Mol Cell Biol 24:5694-709.

Read AP, Newton VE. 1997. Waardenburg syndrome. J Med Genet 34:656-65.

Rehberg S, Lischka P, Glaser G, Stamminger T, Wegner M, Rosorius O. 2002. Sox10 is an active nucleocytoplasmic shuttle protein, and shuttling is crucial for Sox10-mediated transactivation. Mol Cell Biol 22:5826-34.

Remenyi A, Lins K, Nissen LJ, Reinbold R, Scholer HR, Wilmanns M. 2003. Crystal structure of a POU/HMG/DNA ternary complex suggests differential assembly of Oct4 and Sox2 on two enhancers. Genes Dev 17:2048-59.

Sachdev S, Bruhn L, Sieber H, Pichler A, Melchior F, Grosschedl R. 2001. PIASy, a nuclear matrix-associated SUMO E3 ligase, represses LEF1 activity by sequestration into nuclear bodies. Genes Dev 15:3088-103.

Sanchez-Mejias A, Watanabe Y, R MF, Lopez-Alonso M, Antinolo G, Bondurand N, Borrego S. 2010. Involvement of SOX10 in the pathogenesis of Hirschsprung disease: report of a truncating mutation in an isolated patient. J Mol Med 88:507-14.

Schlierf B, Werner T, Glaser G, Wegner M. 2006. Expression of connexin47 in oligodendrocytes is regulated by the Sox10 transcription factor. J Mol Biol 361:11-21.

Sim H, Argentaro A, Harley VR. 2008. Boys, girls and shuttling of SRY and SOX9. Trends Endocrinol Metab 19:213-22.

Staffler A, Hammel M, Wahlbuhl M, Bidlingmaier C, Flemmer AW, Pagel P, Nicolai T, Wegner M, Holzinger A. 2010. Heterozygous SOX9 mutations allowing for residual DNA-binding and transcriptional activation lead to the acampomelic variant of campomelic dysplasia. Hum Mutat 31:E1436-44.

Stolt CC, Rehberg S, Ader M, Lommes P, Riethmacher D, Schachner M, Bartsch U, Wegner M. 2002. Terminal differentiation of myelin-forming oligodendrocytes depends on the transcription factor Sox10. Genes Dev 16:165-70.

Sudbeck P, Scherer G. 1997. Two independent nuclear localization signals are present in the DNA-binding high-mobility group domains of SRY and SOX9. J Biol Chem 272:27848-52.

Thevenet L, Mejean C, Moniot B, Bonneaud N, Galeotti N, Aldrian-Herrada G, Poulat F, Berta P, Benkirane M, Boizet-Bonhoure B. 2004. Regulation of human SRY subcellular distribution by its acetylation/deacetylation. EMBO J 23:3336-45.

Wagner T, Wirth J, Meyer J, Zabel B, Held M, Zimmer J, Pasantes J, Bricarelli FD, Keutel J, Hustert E and others. 1994. Autosomal sex reversal and campomelic dysplasia are caused by mutations in and around the SRY-related gene SOX9. Cell 79:1111-20.

Werner MH, Huth JR, Gronenborn AM, Clore GM. 1995. Molecular basis of human 46X,Y sex reversal revealed from the three-dimensional solution structure of the human SRY-DNA complex. Cell 81:705-14.

Wilson M, Koopman P. 2002. Matching SOX: partner proteins and co-factors of the SOX family of transcriptional regulators. Curr Opin Genet Dev 12:441-6.

Wissmuller S, Kosian T, Wolf M, Finzsch M, Wegner M. 2006. The high-mobility-group domain of Sox proteins interacts with DNA-binding domains of many transcription factors. Nucleic Acids Res 34:1735-44.

Wong J, Farlie P, Holbert S, Lockhart P, Thomas PQ. 2007. Polyalanine expansion mutations in the X-linked hypopituitarism gene SOX3 result in aggresome formation and impaired transactivation. Front Biosci 12:2085-95.

Yokoyama S, Takeda K, Shibahara S. 2006a. Functional difference of the SOX10 mutant proteins responsible for the phenotypic variability in auditory-pigmentary disorders. J Biochem 140:491-9.

Yokoyama S, Takeda K, Shibahara S. 2006b. SOX10, in combination with Sp1, regulates the endothelin receptor type B gene in human melanocyte lineage cells. Febs J 273:1805-20.

Zhu L, Lee HO, Jordan CS, Cantrell VA, Southard-Smith EM, Shin MK. 2004. Spatiotemporal regulation of endothelin receptor-B by SOX10 in neural crest-derived enteric neuron precursors. Nat Genet 36:732-7.

Figure legends

Figure 1. Location of SOX10 missense mutations identified. Schematic representation of the SOX10 protein including the transactivation and HMG DNA binding domains. An alignment presenting amino acid conservation between the HMG domain of SOX10 and that of representative members of several SOX subgroup proteins is shown. Human SOX sequence reference numbers: SOX10 (NP_008872.1), SOX9 (NP_000337.1), SOX17 (NP_071899.1), SOX11 (NP_003099.1), SOX5 (NP_008871.3), SOX2 (NP_003097.1), SOX15 (NP_008873.1), SOX30 (NP_008948.1), and SRY (NP_003131.1). Non-conserved residues are shown in grey, NLSs and NES sequences are underlined, and mutated amino acids are boxed.

Figure 2. DNA binding capacities of the mutant proteins. (A) Western blots presenting mutant proteins production. (B-D) Electrophoretic mobility shift assays using the monomeric binding site "S5" from the *MITF* promoter region (B) or the dimeric binding site "S1S2" from the *Cx32* promoter region (C), and empty pECE vector (-), control (lane 2) or mutant SOX10 proteins (lanes 3 to 13). (D) Electrophoretic mobility shift assay using the C/C' dimeric binding site from the *P0* promoter as a probe and control or p.Met112Ile mutant SOX10 proteins. Increasing amounts (5- to 10-fold molar excess) of unlabeled C'mut oligonucleotide were added as competitor (comp). -, no competitor; m, bound monomer; d, bound dimer.

Figure 3. Transactivation capacities of the mutant proteins. *MITF* (A) or *Cx32* (B) luciferase reporters co-transfected with wild-type or mutant SOX10 and/or PAX3 (A) or EGR2 (B) expression vectors. *RET* enhancer luciferase reporter (C) or *P0* promoter luciferase reporter (D) transfected with wild-type or mutant SOX10 expression vectors. (E) Competition assays. The *Cx32* promoter luciferase reporter plasmid was co-transfected with a fixed amount of wild-type SOX10 and increasing amounts of mutant proteins. In each case, reporter gene activation is presented as fold induction relative to the empty expression vectors. Results represent the mean ± standard error of three to five different experiments, each performed in

duplicate.

Figure 4. Subcellular localization of the mutant proteins. HeLa cells transfected with wild-type or mutant pECE-SOX10 expression vectors were immunostained with SOX10 antibody (red; A2 to L2) or grey (A4 to L4). Cells were counterstained with TO-PRO-3-iodide to visualize nuclei (blue, A1 to L1). A3 to L3 represent merged pictures. White arrowheads indicate nuclear foci.

Figure 5. Quantification of the effect of the mutations on the cellular distribution of SOX10 proteins. (A) Cytoplasmic redistribution was quantified by counting the number of cells presenting with cytoplasmic staining over the total number of transfected cells. (B) The "pool of cells containing foci" was quantified by counting the number of cells presenting a striking nuclear redistribution of SOX10 proteins into punctate structures, relative to the total number of transfected cells. On average, 300 cells per experiment from three different experiments were counted 24 hours post transfection.

Figure 6. Origin of foci formation. (A) Location of the mutations leading to nuclear foci formation and the p.Trp114Val mutation on the HMG domain primary structure. The amino acid substitutions are indicated by arrows and the three helix sequences are indicated. (B) Three-dimensional representation of the HMG domain (SOX17) and its interactions with the target DNA sequence. Four representations are shown. B1: Structural representation of the HMG "L-shape" conformation, made of three helices in which the short arm contains helices 1 and 2 while the long arm is made up of helix 3 and the N-terminus tail. The backbone of the hydrophobic core amino acids is shown in yellow. B2: Same view. The DNA strands are in blue and the HMG backbone in red. Amino acids corresponding to Arg106, Met112, and Asn131, located at the DNA interface, are in green; amino acids Leu145, Lys150, and Ala157 are represented in red; the amino acid corresponding to Arg161 in orange. B3: Structural representation of the general conformation of the HMG domain and DNA helix. For clarity,

the backbone is not shown. The HMG α-helices are in yellow and the N- and C-tails, as well as the DNA strands, are in white. Amino acids corresponding to Gln174 and Pro175 are in red and green, respectively. B4: a different view showing the four amino-acids of the hydrophobic core. The tryptophan located in the α1 helix (Trp114) is in red and the other three are in yellow. (C) Subcellular localization of the p.Trp114Val mutant SOX10 protein. Cells were immunostained with SOX10 antibody (red, C2, or grey, C4) and counterstained with TO-PRO-3-iodide (blue, C1). C3 represents a merged picture. (D) Transactivation capacity of the p.Trp114Val mutant SOX10 proteins. MITF and Cx32 reporter gene activations are presented as fold induction relative to the empty expression vector (pECE). Results represent the mean ± standard error of the mean from three to five different experiments, each performed in duplicate. (E) Stability of wild-type (purple), p.Leu145Pro (blue), p.Lys150Asn (red), and p.Ala157Val (green) were compared in HeLa transfected cells cultured for various times in the presence of cycloheximide as indicated, and SOX10 proteins detected by Western. Relative amount of proteins were quantified from band intensities with the amount in untreated cells set to 100%. Half life of wild-type and p.Leu145Pro, p.Lys150Asn, and p.Ala157Val were 6, 6, 8 and 7 hours respectively.

Case	Nucleotide change	Protein (predicted)	Inheritance	Gender	Age	Phenotype	depigmentation hearing loss	Intestinal	Neurological	References
A	**c.316C>T**	**p.Arg106Trp**	**ND**	**F**	**20**	**WS4**	**+**	**HD**	**-**	**This paper**
B	**c.336G>A**	**p.Met112Ile**	**de novo**	**M**	**1**	**PCWH**	**+**	**HD**	**+**	**This paper**
C	**c.336G>A**	**p.Met112Ile**	**de novo**	**M**	**7 M**	**PCW or PCWH**	**+ (hypoacousia one side)**	**temporary constipation**	**+**	**This paper**
D	**c.336G>C**	**p.Met112Ile**	**familial**	**F/F**	**43/13**	**WS2 (2/2)**	**+ (2/2)**	**-**	**-**	**This paper**
E	**c.391A>C**	**p.Asn131His**	**de novo**	**M**	**2**	**PCWH**	**+**	**HD**	**+**	**This paper**
F	**c.434T>C**	**p.Leu145Pro**	**? (Father not tested)**	**M**	**3.5**	**WS4**	**+**	**HD**	**-**	**This paper**
G	**c.[450G>C(+)961G>C]**	**p.[Lys150Asn(+)Gly321Arg]**	**de novo**	**M**	**4**	**PCWH**	**+**	**HD**	**+**	**This paper**
H	c.470C>T	p.Ala157Val	de novo	M	18 M	WS4	+	HD	-	(Morin et al., 2008)
I	**c.482G>A**	**p.Arg161His**	**ND**	**M**	**2**	**WS2**	**+**	**-**	**-**	**This paper**
J	c.521A>C	p.Gln174Pro	?	M	18 M	PCW	+	-	+	(Barnett et al., 2009)
K	**c.523C>G**	**p.Pro175Ala**	**de novo**	**F**	**11**	**PCWH**	**+**	**po**	**+**	**This paper**
L	**c.524C>T**	**p.Pro175Leu**	**familial**	**F/3M**	**50/44/11/10**	**PCW (4/4)**	**+ (4/4)**	**-**	**+ (4/4)**	**This paper**
M	**c.524C>G**	**p.Pro175Arg**	**de novo**	**M**	**30**	**PCWH**	**+**	**constipation**	**+**	**This paper**

Table 1: Summary of missense mutations identified and clinical findings. Mutations indicated in bold are new identified mutations. Non bold mutations were previously published (see references). cDNA numbering follows the reference NM_006941.3. Two familial cases are reported (D and L). Gender, age and phenotype of each family member are reported. HD= Hirschsprung; WS=Waardenburg syndrome; po= intestinal pseudo obstruction. M: Months; ND=Not Determined.

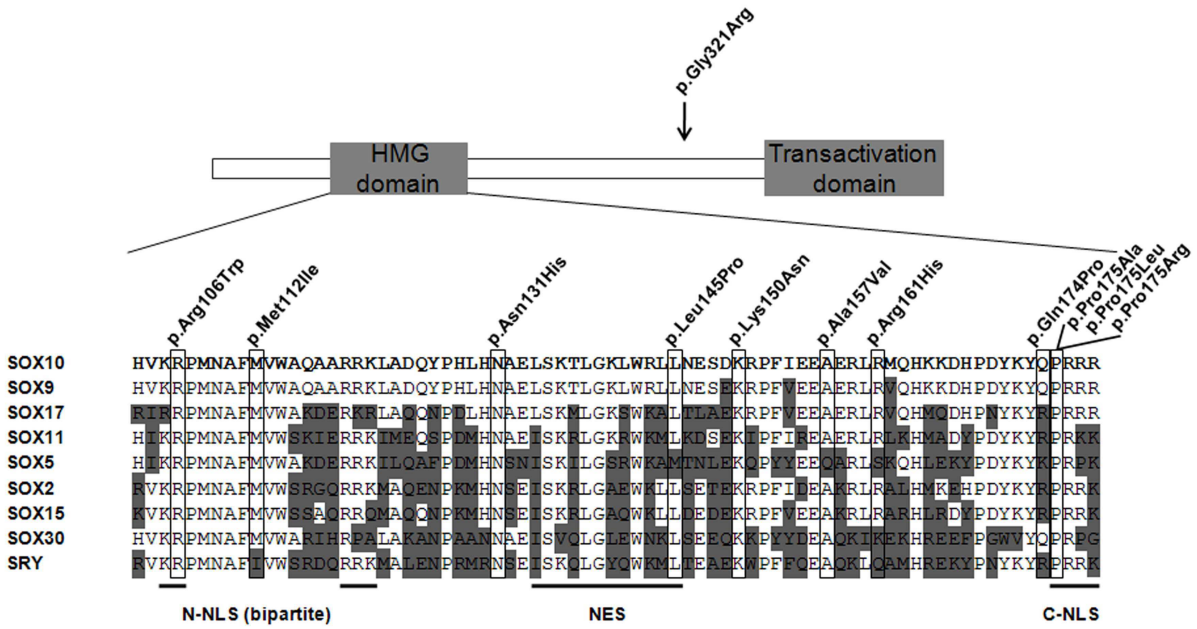
p.Gly321Arg
HMG domain
Transactivation domain
p.Arg106Trp
p.Met112Ile
p.Asn131His
p.Leu145Pro
p.Lys150Asn
p.Ala157Val
p.Arg161His
p.Gln174Pro
p.Pro175Ala
p.Pro175Leu
p.Pro175Arg
SOX10
SOX9
SOX17
SOX11
SOX5
SOX2
SOX15
SOX30
SRY
N-NLS (bipartite)
NES
C-NLS

Figure1

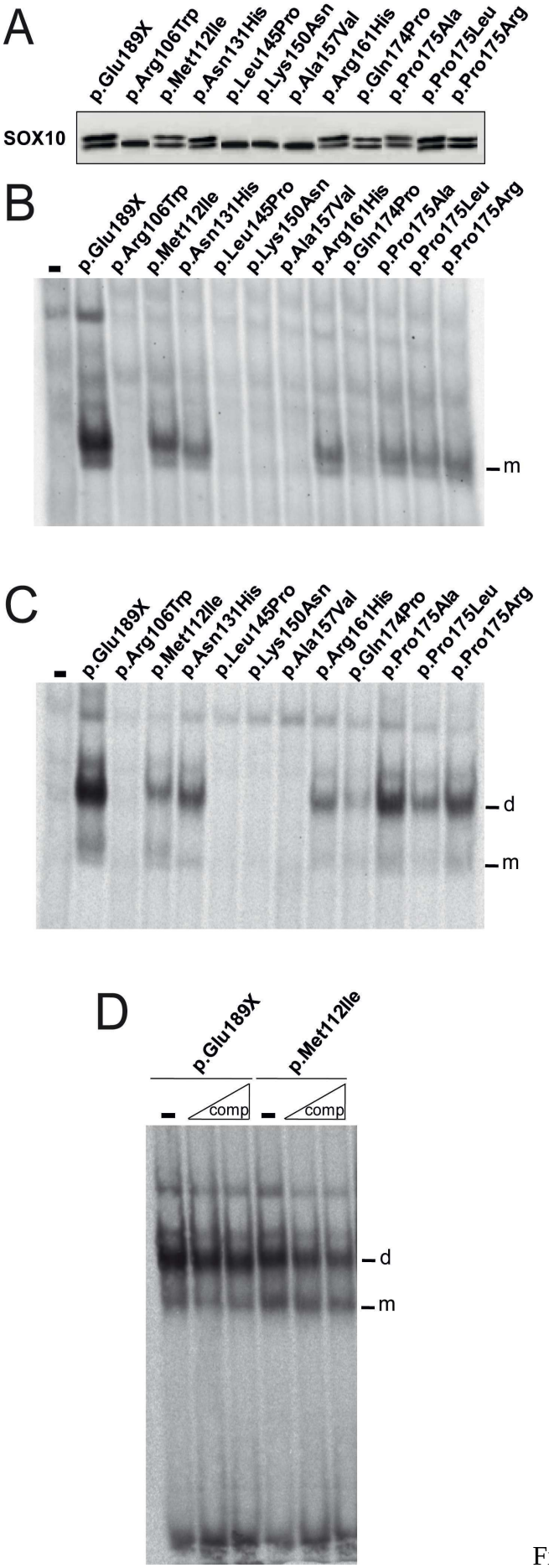
A
p.Glu189X
p.Arg106Trp
p.Met112Ile
p.Asn131His
p.Leu145Pro
p.Lys150Asn
p.Ala157Val
p.Arg161His
p.Gln174Pro
p.Pro175Ala
p.Pro175Leu
p.Pro175Arg
SOX10
B
-
p.Glu189X
p.Arg106Trp
p.Met112Ile
p.Asn131His
p.Leu145Pro
p.Lys150Asn
p.Ala157Val
p.Arg161His
p.Gln174Pro
p.Pro175Ala
p.Pro175Leu
p.Pro175Arg
m
C
-
p.Glu189X
p.Arg106Trp
p.Met112Ile
p.Asn131His
p.Leu145Pro
p.Lys150Asn
p.Ala157Val
p.Arg161His
p.Gln174Pro
p.Pro175Ala
p.Pro175Leu
p.Pro175Arg
d
m
D
p.Glu189X
p.Met112Ile
-
comp
-
comp
d
m

Figure 2

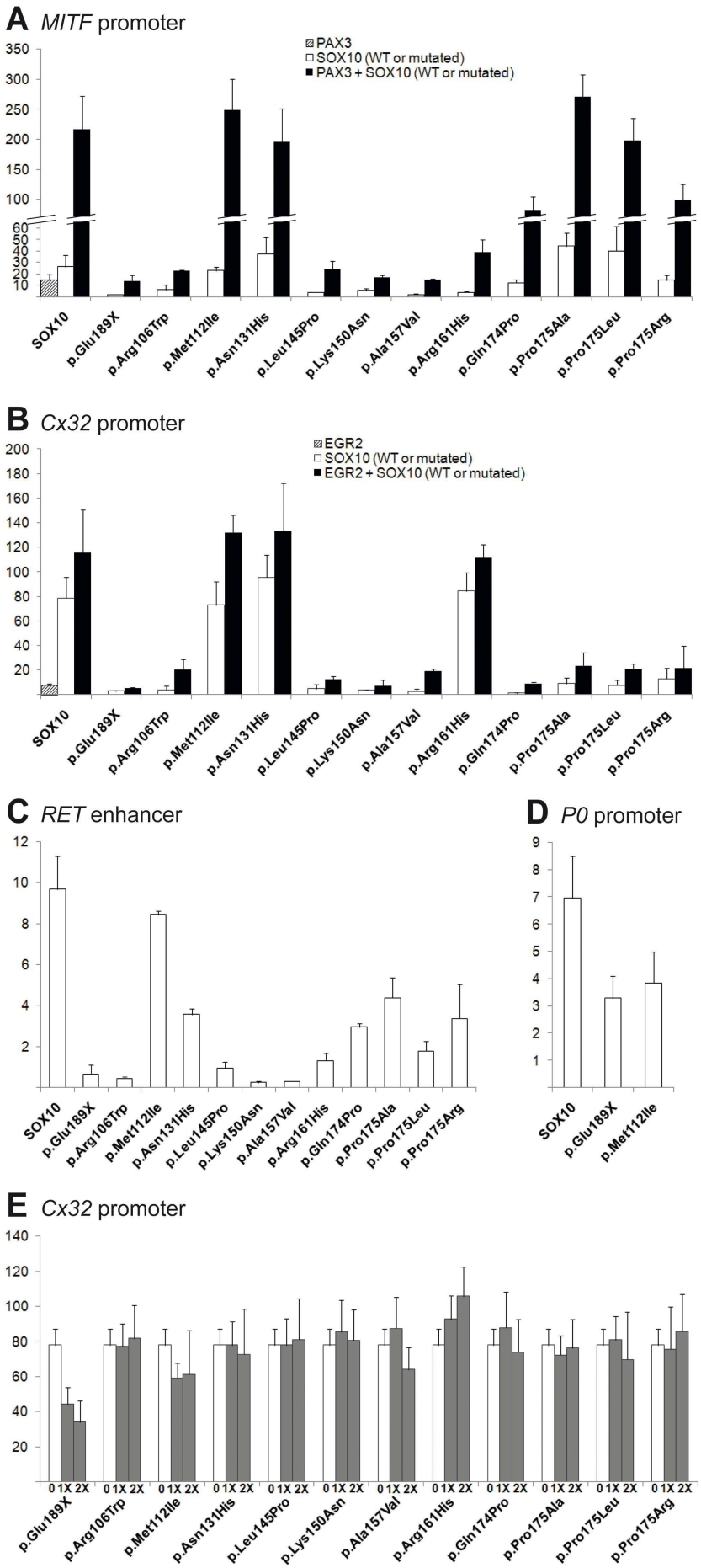
A MITF promoter
PAX3
SOX10 (WT or mutated)
PAX3 + SOX10 (WT or mutated)
B Cx32 promoter
EGR2
SOX10 (WT or mutated)
EGR2 + SOX10 (WT or mutated)
C RET enhancer
D P0 promoter
E Cx32 promoter
SOX10
p.Glu189X
p.Arg106Trp
p.Met112Ile
p.Asn131His
p.Leu145Pro
p.Lys150Asn
p.Ala157Val
p.Arg161His
p.Gln174Pro
p.Pro175Ala
p.Pro175Leu
p.Pro175Arg
0 1X 2X

Fgure3

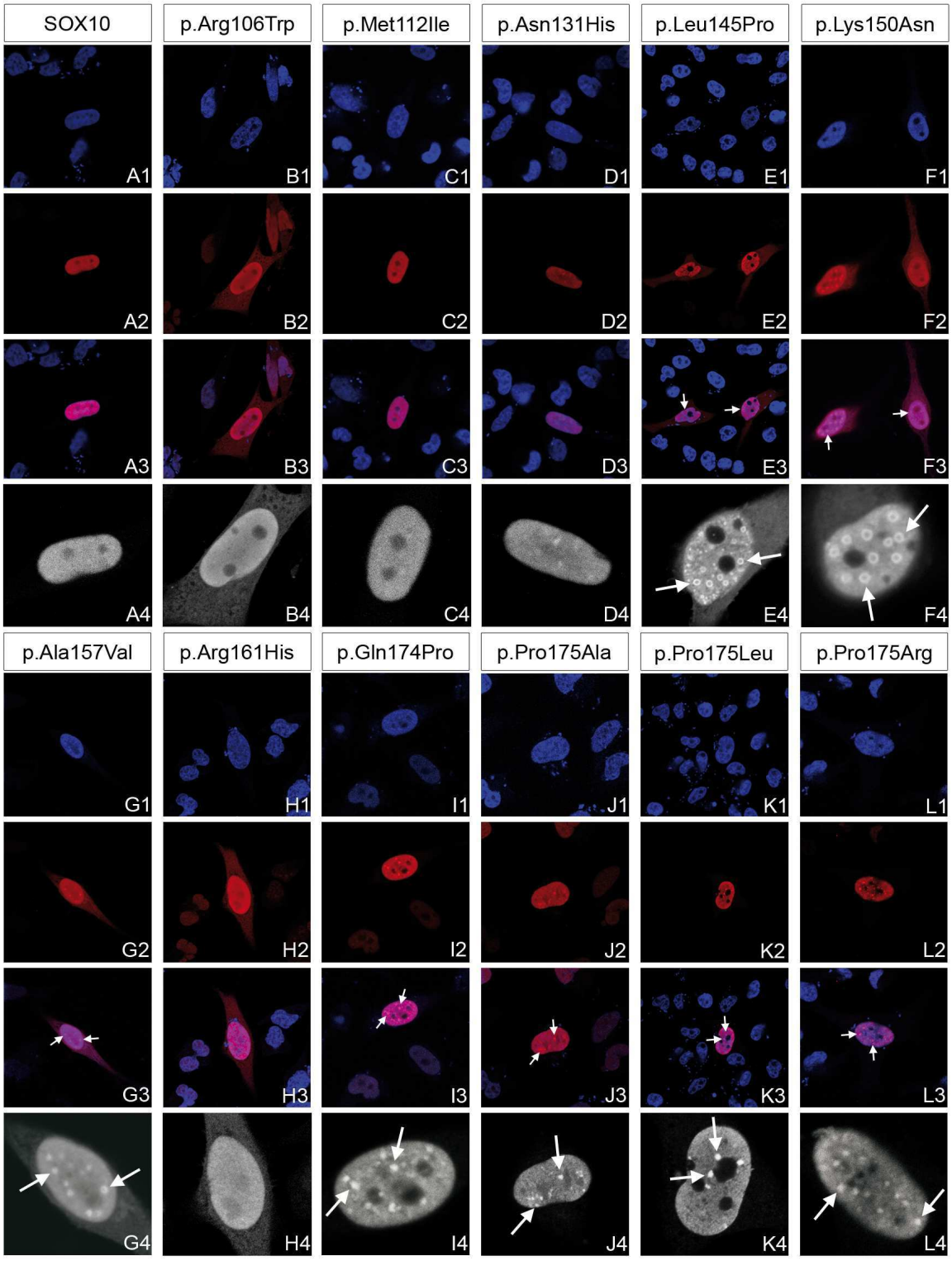
SOX10
p.Arg106Trp
p.Met112Ile
p.Asn131His
p.Leu145Pro
p.Lys150Asn
A1
B1
C1
D1
E1
F1
A2
B2
C2
D2
E2
F2
A3
B3
C3
D3
E3
F3
A4
B4
C4
D4
E4
F4
p.Ala157Val
p.Arg161His
p.Gln174Pro
p.Pro175Ala
p.Pro175Leu
p.Pro175Arg
G1
H1
I1
J1
K1
L1
G2
H2
I2
J2
K2
L2
G3
H3
I3
J3
K3
L3
G4
H4
I4
J4
K4
L4

Figure4

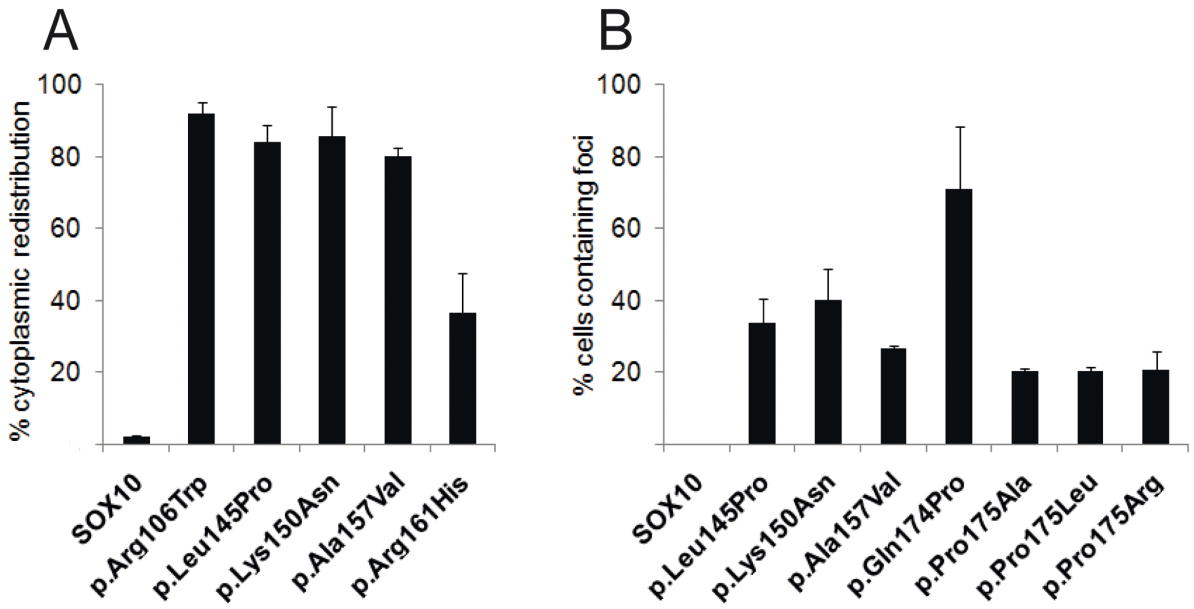
A
% cytoplasmic redistribution
100
80
60
40
20
SOX10
p.Arg106Trp
p.Leu145Pro
p.Lys150Asn
p.Ala157Val
p.Arg161His
B
% cells containing foci
100
80
60
40
20
SOX10
p.Leu145Pro
p.Lys150Asn
p.Ala157Val
p.Gln174Pro
p.Pro175Ala
p.Pro175Leu
p.Pro175Arg

Figure5

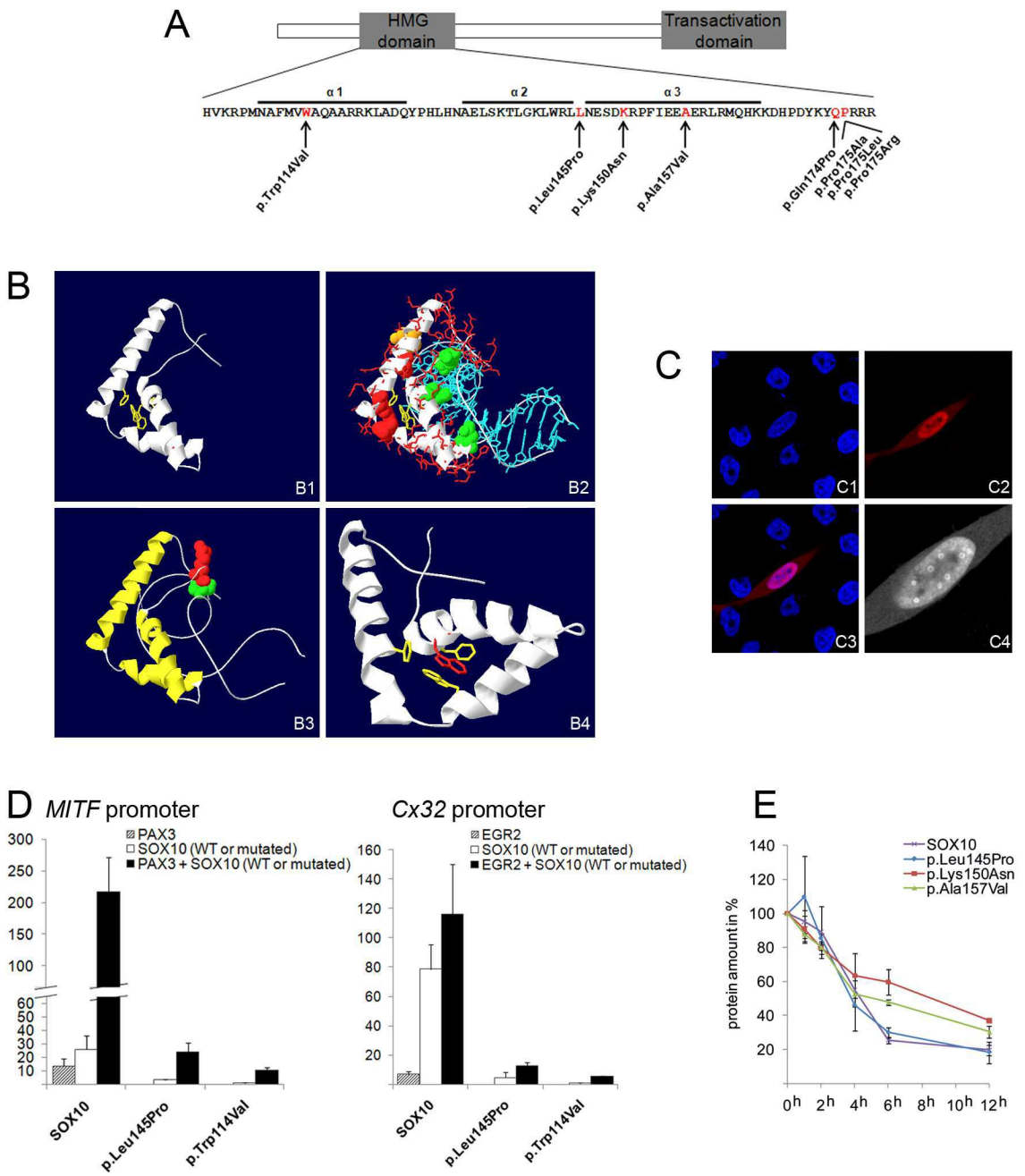
A
HMG domain
Transactivation domain
α 1
α 2
α 3
HVKRPMNAFMVWAQAARRKLADQYPHLHNAELSKTLGKLWRLLNESDKRPFIEEAERLRMQHKKDHPDYKYQPRRR
p.Trp114Val
p.Leu145Pro
p.Lys150Asn
p.Ala157Val
p.Gln174Pro
p.Pro175Ala
p.Pro175Leu
p.Pro175Arg
B
B1
B2
B3
B4
C
C1
C2
C3
C4
D
MITF promoter
PAX3
SOX10 (WT or mutated)
PAX3 + SOX10 (WT or mutated)
SOX10
p.Leu145Pro
p.Trp114Val
Cx32 promoter
EGR2
SOX10 (WT or mutated)
EGR2 + SOX10 (WT or mutated)
SOX10
p.Leu145Pro
p.Trp114Val
E
SOX10
p.Leu145Pro
p.Lys150Asn
p.Ala157Val
protein amount in %
0h
2h
4h
6h
8h
10h
12h

Figure6

Supplementary figures:

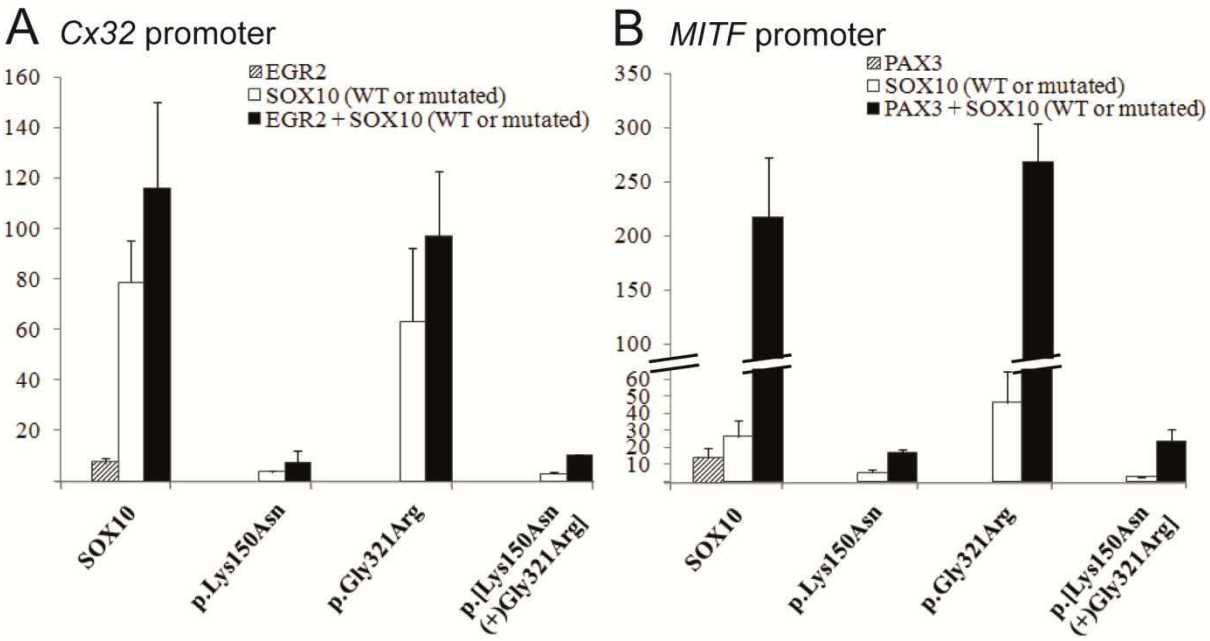

Supp.Figure S1. Transactivation capacity of the p.[Lys150Asn(+)Gly321Arg] mutant SOX10 protein. The *Cx32* (A) or *MITF* (B) reporter constructs were transfected in HeLa cells in combination with the empty pECE vector, wild type, p.Lys150Asn, p.Gly321Arg or p.[Lys150Asn(+)Gly321Arg] mutants, and/or EGR2 (A) or PAX3 (B). Reporter gene activation is presented as fold induction relative to the empty vector. Results represent the mean ± standard error of three to five different experiments, each performed in duplicate.

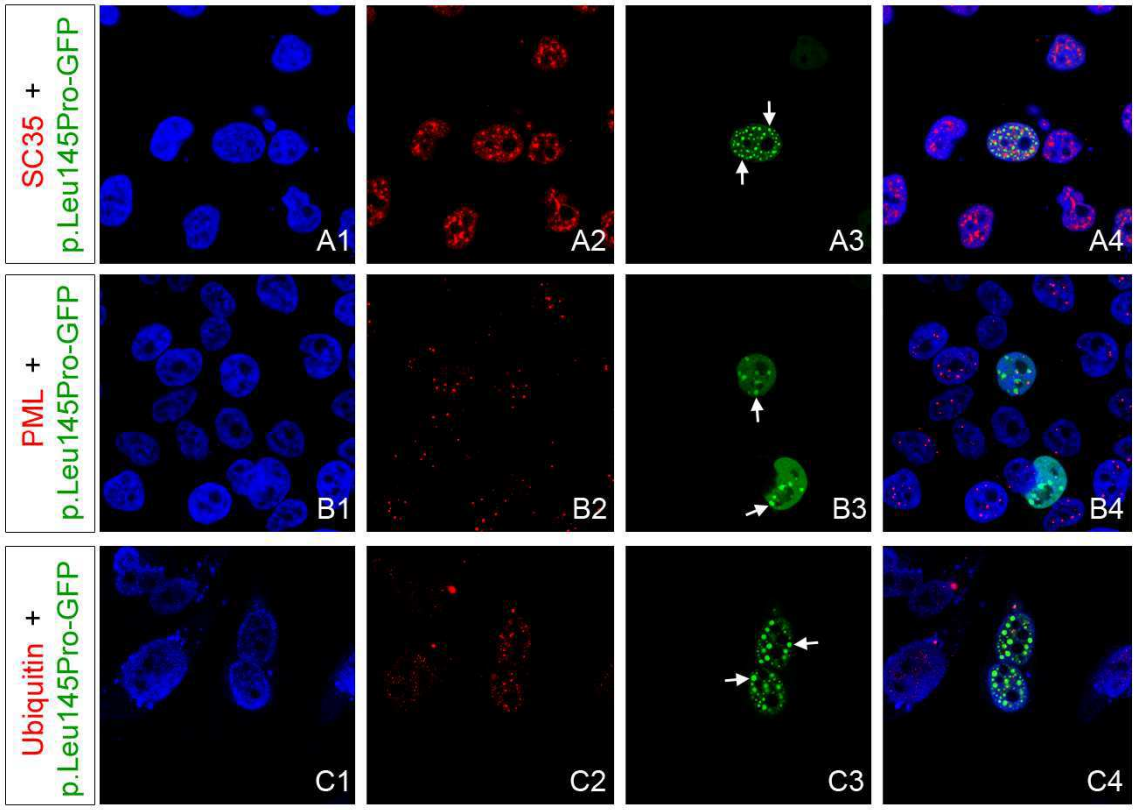

Supp.Figure S2. Characterization of nuclear foci. HeLa cells were transfected with the p.Leu145Pro mutated version of SOX10-GFP expression vector and immunostained with various markers such as SC35 (A1 to A4), PML (B1 to B4), and ubiquitin (C1 to C4). Cells were counterstained with TO-PRO-3-iodide to visualize nuclei (blue, A1 to C1). A4 to C4 represent merged pictures. White arrows indicate nuclear foci. Antibodies used are as follow: PML PG-M3 (mouse; Santa Cruz Biotechnology, INC., Santa Cruz, CA, USA) 1:10; SC35 (mouse; Sigma, St Louis, MO, USA) 1:50; Ub P4D1 (mouse; Santa Cruz Biotechnologies, INC., Santa Cruz, CA, USA) 1:50.

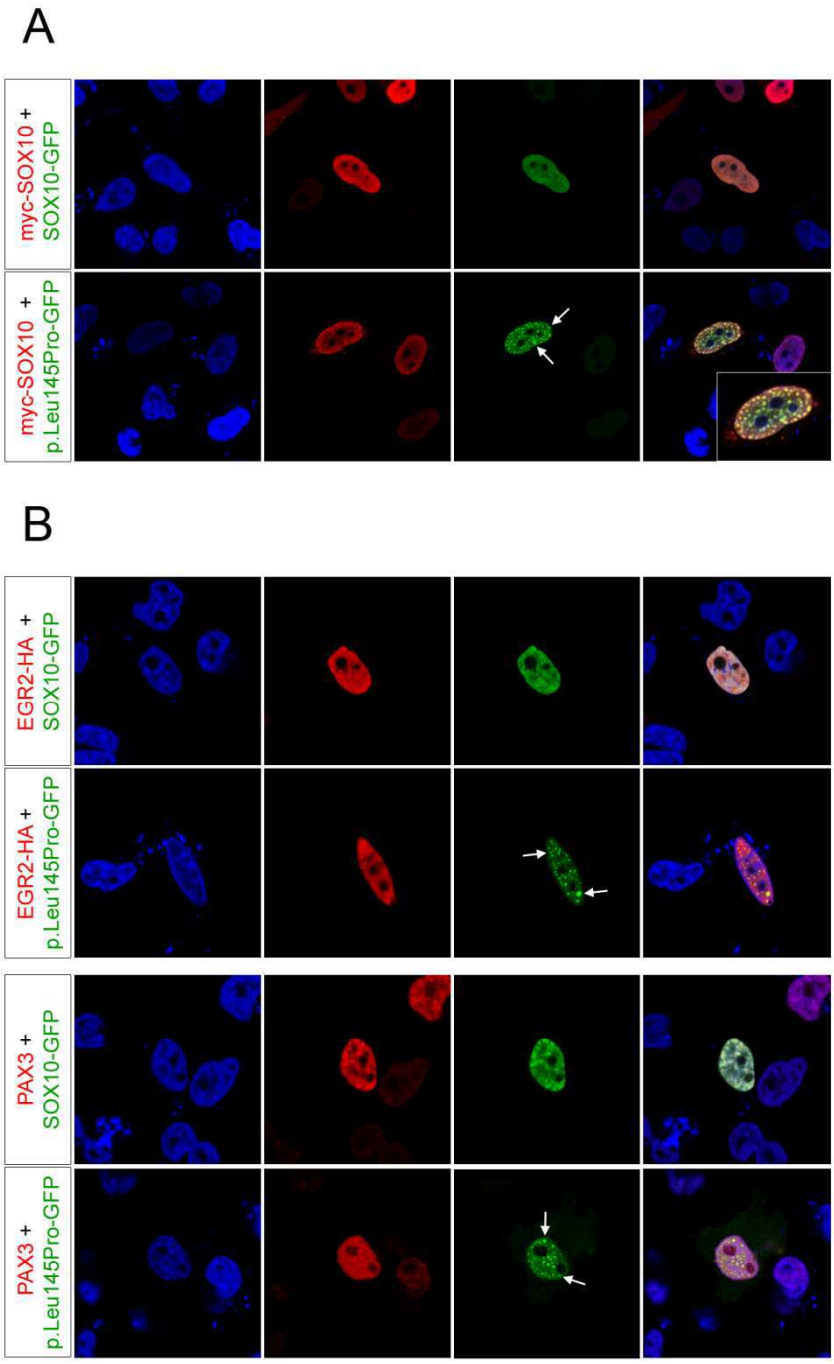

Supp.Figure S3. The SOX10 mutants recruit wild-type SOX10 protein but not its cofactors within foci. (A) The intracellular distribution of a myc-tagged version of wild-type SOX10 (red) was compared with that of wild-type or the p.Leu145Pro mutated version of SOX10-GFP (green) after co-transfection. (B) The wild-type or p.Leu145Pro mutated version

of SOX10-GFP expression vector co-transfected with the expression vector encoding EGR2-HA or PAX3 cofactors to compare their intracellular distribution. Cells were counterstained with TO-PRO-3-iodide to visualize nuclei (blue). White arrows indicate nuclear foci. Antibodies used are as follow: anti-HA (C12CA5; Roche Applied Science, Indianapolis, IN, USA) 1:75; The PAX3 and myc (9E10) monoclonal antibodies developed by Charles P. Ordahl and J. Michael Bishop were obtained from the Developmental Studies Hybridoma Bank under the auspices of the NICHD and maintained by the University of Iowa, Department of Biology, Iowa City, IA 52242, and used at 1:200 and 1:50 dilutions, respectively.